Spin relaxation of conduction electrons in bulk III-V semiconductors

Pil Hun Song and K. W. Kim*
Department of Electrical and Computer Engineering, North Carolina State University, Raleigh, North Carolina 27695-7911
(Received 5 November 2001; published 31 July 2002)

The spin relaxation time of conduction electrons through the Elliot-Yafet, D'yakonov-Perel, and Bir-Aronov-Pikus mechanisms is calculated theoretically for bulk GaAs, GaSb, InAs, and InSb of both *n* and *p* type. The relative importance of each spin relaxation mechanism is compared, and diagrams showing the dominant mechanism are constructed as a function of the temperature and impurity concentration. Our approach is based upon theoretical calculations of the momentum relaxation rate, and allows one to understand the interplay between various factors affecting the spin relaxation over a broad range of temperature and impurity concentration.

DOI: 10.1103/PhysRevB.66.035207 PACS number(s): 72.25.Rb, 76.20.+q, 76.60.Es

I. INTRODUCTION

Recently, intensive experimental and theoretical efforts have been concentrated on the physics of electron spins due to the enormous potential of spin-based devices. In these so-called ''spintronic'' devices,[1–3] information is encoded in the spin state of individual electrons, transferred with the electrons, and finally put under measurement. Electron-spin states relax (depolarize) by scattering with imperfections or elementary excitations such as other carriers and phonons. Therefore, to realize any useful spintronic devices, it is essential to understand and have control over spin relaxation such that the information is not lost before a required operation is completed.

The investigation of spin relaxation has a long history dating back to the 1950s. Most studies concentrated on III-V semiconductors, since a direct measurement of spin relaxation time is possible through an optical orientation in these materials. Three main spin relaxation mechanisms, the Elliot-Yafet[4,5] (EY), D'yakonov-Perel[6] (DP) and Bir-Aronov-Pikus[7] (BAP) mechanisms were suggested and confirmed experimentally. Earlier works for spin relaxation concentrated mainly on bulk systems such as *p*-GaAs,[8–11] *p*-GaSb,[12] GaAlAs,[13] and *n*-InSb.[14] More recently, spin relaxation was also investigated in quantum well structures [GaAs,[15] GaAsSb,[16] InGaAs/InGaAsP,[17] and GaAs/AlGaAs (Ref. 18)] as well as in bulk systems [*n*-GaAs (Refs. 19 and 20) and InAs (Ref. 21)]. On the theoretical side, there are recent approaches which refine or extend the original calculations of Refs. 6 and 7 to explain newly obtained experimental results. Flatté and co-workers[21,22] employed a nonperturbative 14-band calculation for the DP mechanism both for bulk and quantum-well structures, and achieved better agreement with the experimental results. The BAP process was reconsidered through a direct Monte Carlo simulation, and extended to quantum wells by Maialle and co-workers.[23]

In most studies, the strategy has been to find the relevant spin relaxation mechanism by comparing experimental results for the spin relaxation time τ_s with the theoretically predicted dependence on temperature or doping concentrations. Based upon these results, a ''phase diagram-like'' picture showing the dominant spin relaxation mechanism can be constructed to provide a comprehensive global understanding for a competition between spin relaxation mechanisms. However, since available experimental results for τ_s are usually limited to a narrow range of external physical parameters except for some intensively investigated materials, such pictures are currently available only for *p*-GaAs and *p*-GaSb.[12]

In this paper, we calculate the electron spin relaxation time for the EY (τ_s^{EY}), DP (τ_s^{DP}), and BAP (τ_s^{BAP}) processes for several bulk III-V semiconductors: GaAs, GaSb, InAs, and InSb of both *n* and *p* types. Our result for τ_s is based upon a theoretical calculation of the momentum relaxation time τ_p. A diagram is constructed illustrating the dominant spin relaxation processes as a function of temperature and impurity concentration for each material. The resulting ''phase diagrams'' for *p*-GaAs and *p*-GaSb are in qualitative agreement with that of an earlier study.[12] The diagrams for the other materials considered in this work were not available in the literature, and represent an attempt to provide a better understanding of interplay between various factors for τ_s. We also discuss some incomplete aspects of the current theories for spin relaxation.

The rest of this paper is organized as follows. In Sec. II the basic formulation of the three spin relaxation mechanisms is briefly described. The details of our calculation for the momentum relaxation time (τ_p) and τ_s are presented in Sec. III. In Sec. IV the results for τ_s are compared with available experimental results and the ''phase diagrams'' for dominant spin relaxation is constructed. The conclusion follows in Sec. IV.

II. RELEVANT SPIN RELAXATION MECHANISMS

A. Elliot-Yafet mechanism

The EY mechanism originates from the fact that, in the presence of spin-orbit coupling, the exact Bloch state is not a spin eigenstate but a superposition of them. This induces a finite probability for spin flip when the spatial part of electron wave function experiences a transition through scattering even if the involved interaction is spin independent.[4,5] The spin relaxation time is given by[24]

$$\frac{1}{\tau_s^{EY}} = A\left(\frac{k_B T}{E_g}\right)^2 \eta^2 \left(\frac{1-\eta/2}{1-\eta/3}\right)^2 \frac{1}{\tau_p}, \tag{1}$$

where E_g is the band gap and $\eta = \Delta/(E_g+\Delta)$ with the spin-orbit splitting of the valence band Δ. A is a dimensionless constant and varies from 2 to 6 depending on the dominant scattering mechanism for momentum relaxation.

B. D'yakonov-Perel mechanism

In III-V semiconductors, the degeneracy in the conduction band is lifted for $\mathbf{k} \neq 0$ due to the absence of inversion symmetry. The resulting energy difference, for electrons with the same $\mathbf{k}$ but different spin states, plays the role of an effective magnetic field and results in spin precession with angular velocity $\omega(\mathbf{k})$ during the time between collisions. Since the magnitude and the direction of $\mathbf{k}$ changes in an uncontrolled way due to electron scattering with impurities and excitations, this process contributes to spin relaxation. This is called the DP mechanism,[6] and τ_s^{DP} is given by[6,24]

$$\frac{1}{\tau_s^{DP}} = Q\alpha^2 \frac{(k_B T)^3}{\hbar^2 E_g} \tau_p, \tag{2}$$

where Q is a dimensionless factor and ranges from 0.8 to 2.7 depending on the dominant momentum relaxation process. α is the parameter characterizing the k^3 term for conduction-band electrons, and is approximately given by[12]

$$\alpha \simeq \frac{4\eta}{\sqrt{3-\eta}} \frac{m_c}{m_0}. \tag{3}$$

Here m_c and m_0 are the effective mass of the conduction electron and the electron rest mass, respectively.

C. Bir-Aronov-Pikus mechanism

The electron spin-flip transition is also made possible by electron-hole scattering via exchange and annihilation interactions. This is called the BAP mechanism, and is especially strong in p-type semiconductors due to high hole concentrations. τ_s^{BAP} is given by several different expressions depending on the given external parameters. In the case of a nondegenerate semiconductor[7,24] ($N_A < N_c$),

$$\frac{1}{\tau_s^{BAP}} = \frac{2a_B^3}{\tau_0 v_B}\left(\frac{2\epsilon}{m_c}\right)^{1/2}\left[n_{a,f}|\psi(0)|^4 + \frac{5}{3} n_{a,b}\right], \tag{4}$$

where $n_{a,f}$ ($n_{a,b}$) is the concentration of free (bound) holes and N_c is the critical hole concentration between degeneracy and nondegeneracy. ϵ is the conduction electron energy, and τ_0 is given by the relation

$$\frac{1}{\tau_0} = \frac{3\pi}{64} \frac{\Delta_{exc}^2}{E_B \hbar},$$

with Δ_{exc} the exchange splitting of the exciton ground state. a_B, v_B and E_B are defined as

$$a_B = \frac{\hbar^2 \epsilon_0}{e^2 m_R} = \left(\frac{m_0}{m_R}\right)\epsilon_0 a_0,$$

$$v_B = \frac{\hbar}{m_R a_B},$$

$$E_B = \frac{\hbar^2}{2m_R a_B^2} = \left(\frac{m_R}{m_0}\right)\frac{\mathcal{R}}{\epsilon_0^2},$$

where m_R is the reduced mass of electron and hole, a_0 the Bohr radius ($\simeq 0.53$ Å), and $\mathcal{R}$ the Rydberg constant ($\simeq 13.6$ eV). $\psi(\mathbf{r})$ represents wavefunction describing the relative motion of electron with respect to hole and $|\psi(0)|^2$ is the Sommerfeld factor given by

$$|\psi(0)|^2 = \frac{2\pi}{\kappa}(1-e^{-2\pi/\kappa})^{-1}, \quad \kappa = \sqrt{\frac{\epsilon}{E_B}}.$$

For the degenerate case ($N_A > N_c$), the result is[7,24]

$$\frac{1}{\tau_s^{BAP}} = \frac{2a_B^3}{\tau_0 v_B}\left(\frac{\epsilon}{\epsilon_f}\right) N_A |\psi(0)|^4 \times \begin{cases} (2\epsilon/m_c)^{1/2} & \text{if } \epsilon_f < \epsilon(m_v/m_c) \\ (2\epsilon_f/m_v)^{1/2} & \text{if } \epsilon_f > \epsilon(m_v/m_c), \end{cases} \tag{5}$$

where m_v is the hole effective mass and ϵ_f the hole Fermi energy, $(\hbar^2/2m_h)(3\pi^2 N_A)^{2/3}$.

III. CALCULATION

We first calculate the momentum relaxation time τ_p. We include contributions from polar optical phonon scattering (τ_p^{po}), ionized impurity scattering (τ_p^{ii}), piezoelectric scattering (τ_p^{pe}), and acoustic phonon deformation potential scattering (τ_p^{dp}). Our calculation of τ_p is performed with three simplifying assumptions: (a) the classical Boltzmann statistics is assumed for conduction electrons, (b) the electrons are scattered in a parabolic band, and (c) Mathiessen's rule is applied so that $1/\tau_p = 1/\tau_p^{po} + 1/\tau_p^{ii} + 1/\tau_p^{pe} + 1/\tau_p^{dp}$. Under these assumptions, τ_p can be obtained in a straightforward way for the given material parameters of a III-V semiconductor.

According to the Ehrenreich's variational calculation,[25] τ_p^{po} is obtained as

$$\tau_p^{po} = \frac{4}{3\sqrt{\pi}} \frac{\hbar}{\sqrt{\mathcal{R} k_B T}}\left(\frac{\epsilon_0 \epsilon_\infty}{\epsilon_0 - \epsilon_\infty}\right)\left(\frac{m_0}{m_c}\right)^{1/2} \frac{e^{\theta_l/T}-1}{\theta_l/T} G^{(1)} e^{-\xi}, \tag{6}$$

where ϵ_0 and ϵ_∞ are the low- and high-frequency dielectric constants. θ_l is the longitudinal optical phonon frequency converted in units of temperature and $G^{(1)}e^{-\xi}$ is calculated as in Ref. 26 as a function of temperature and the free-carrier density n.

τ_p^{ii} is described by the Brooks-Herring equation[27]

TABLE I. Material parameters. N_c is from the relation $N_c \approx (0.26/a_H)^3$ and all other numbers are from Ref. 35 unless specified otherwise.

	GaAs	GaSb	InAs	InSb
m_c/m_0	0.065	0.0412	0.023	0.0136
m_v/m_0	0.5	0.28	0.43	0.45
Δ (eV)	0.341	0.75	0.38	0.85
$E_{g,l}$ (eV)	1.52 (0 K)	0.822 (0 K)	0.418 (4.2 K)	0.235 (1.8 K)
$E_{g,h}$ (eV)	1.42 (300 K)	0.75 (300 K)	0.354 (295 K)	0.23 (77 K)
ϵ_0	12.515	15.69	15.15	16.8
ϵ_∞	10.673	14.44	12.25	15.68
θ_l (K)	410	335	343	280
c_{11} (dyn/cm^2)	1.221×10^{12}	8.834×10^{11}	8.329×10^{11}	6.669×10^{11}
c_{12} (dyn/cm^2)	5.66×10^{11}	4.023×10^{11}	4.526×10^{11}	3.645×10^{11}
c_{44} (dyn/cm^2)	5.99×10^{11}	4.322×10^{11}	3.959×10^{11}	3.02×10^{11}
h_{14} (V/cm)	1.45×10^{7}	9.5×10^{6}	3.5×10^{6}	4.7×10^{6}
E_1 (eV)	6.3[a]	6.7[b]	4.9[b]	7.2[b]
Δ_{exc} (μeV)	50[c]	24[d]	unknown	unknown
N_c (cm^{-3})	7.53×10^{18}	6.71×10^{17}	2.7×10^{18}	2.27×10^{18}

[a]Reference 36.
[b]Reference 34.
[c]Reference 37.
[d]Reference 12.

$$\tau_p^{ii} = \frac{1}{3\pi^{3/2}} \frac{\epsilon_0^2/a_0^3}{2N_m+n} \frac{\hbar (k_B T)^{3/2}}{\mathcal{R}^{5/2}} \left(\frac{m_c}{m_0}\right)^{1/2} \int_0^\infty \frac{x^3 e^{-x}}{g(n,T,x)} dx, \tag{7}$$

where N_m is the concentration of minority impurities, i.e., acceptors for *n*-type materials and donors for *p*-type materials and x is a dimensionless quantity representing $(\epsilon/k_B T)$. $g(n,T,x)$ is given by

$$g(n,T,x) = \ln(1+b) - b/(1+b),$$

with

$$b = \frac{1}{2\pi} \frac{\epsilon_0}{a_0^3 n} \left(\frac{k_B T}{\mathcal{R}}\right)^2 \left(\frac{m_c}{m_0}\right) x.$$

τ_p^{pe} is given by[28]

$$\tau_p^{pe} = \frac{280\sqrt{\pi}}{3} \frac{\hbar}{\sqrt{\mathcal{R} k_B T}} \left(\frac{m_0}{m_c}\right)^{1/2} \frac{\mathcal{R} a_0/e^2}{h_{14}^2 (4/c_t + 3/c_l)}, \tag{8}$$

after a spherical average of the piezoelectric and elastic constants over the zinc-blende structure is performed.[29] Here h_{14} is the one independent piezoelectric constant, and c_l and c_t are the average longitudinal and transverse elastic constants given by

$$c_l = (3c_{11} + 2c_{12} + 4c_{44})/5,$$

$$c_t = (c_{11} - c_{12} + 3c_{44})/5.$$

Finally, Bardeen and Shockley[30] showed that τ_p^{dp} is given by

$$\tau_p^{dp} = \frac{8\sqrt{\pi}}{3} \frac{\hbar \mathcal{R}^{5/2}}{E_1^2 (k_B T)^{3/2}} \left(\frac{m_0}{m_c}\right)^{3/2} \frac{a_0^3 c_l}{\mathcal{R}}, \tag{9}$$

where E_1 is the deformation potential.

The free-carrier concentration n (i.e., electrons for *n*-type materials and holes for *p*-type materials) is calculated from the equation

$$\frac{n(n+N_m)}{N_M - N_m - n} = \frac{N(T)}{2} \exp\left(\frac{-E_i}{k_B T}\right). \tag{10}$$

Here N_M is the majority impurity concentration. $N(T)$ is given by $[2mk_B T/(\pi\hbar^2)]^{3/2}/4$, where m represents m_c for *n*-type materials and m_v for *p*-type materials, respectively. E_i is the ionization energy for the majority impurity, and is given by $(\mathcal{R}/\epsilon_0^2)(m/m_0)$.

Table I shows the values of material parameters used in the calculation of τ_p and τ_s. $E_g(T)$ is obtained by linearly interpolating or extrapolating $E_{g,l}$ and $E_{g,h}$. N_m is fixed to 5×10^{13} cm^{-3} in most cases. Figure 1 shows the results of mobility calculation, $\mu = (e/m_c)\tau_p$, for *n*-GaAs and *n*-InAs. Good agreement is obtained with the published result of Rode and Knight[33] for *n*-GaAs, while the result for *n*-InAs shows a larger discrepancy up to $\sim$50% with those of Rode.[34] This seems to result from the fact that the nonparabolicity of conduction band, which we neglected, is stronger in InAs.

Figure 2 illustrates the dominant momentum relaxation mechanism for *n*-GaAs as a function of temperature and impurity concentration. It is found that the contribution from polar optical phonon scattering is dominant for the high-T and lightly doped regimes, while ionized impurity scattering

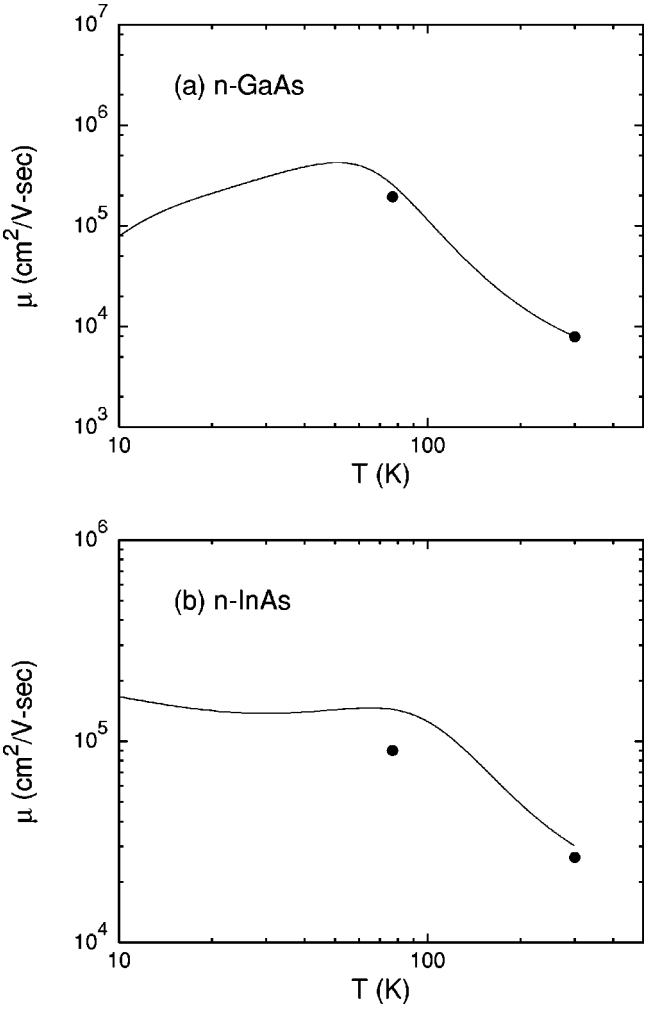

FIG. 1. Mobility vs temperature for (a) *n*-GaAs for $N_D = 10^{14}$ cm^{-3} and $N_A = 5\times10^{13}$ cm^{-3} and (b) *n*-InAs for $N_D = 2\times10^{16}$ cm^{-3} and $N_A = 5\times10^{13}$ cm^{-3}. The lines are our calculation and the points are from (a) Rode and Knight (Ref. 33) and (b) Rode (Ref. 34).

dominates otherwise. The same qualitative features are found for all other materials investigated, both for *n*- and *p*-type cases.

As was noted previously, both τ_s^{EY} and τ_s^{DP} include dimensionless factors, A in Eq. (1) and Q in Eq. (2), which vary depending on the dominant momentum relaxation process. These variations might be numerically calculated when one employs the Mathiessen's rule for given electron energy as

$$1/\tau_p(\epsilon) = 1/\tau_p^{po}(\epsilon) + 1/\tau_p^{ii}(\epsilon) + 1/\tau_p^{pe}(\epsilon) + 1/\tau_p^{dp}(\epsilon).$$

Unfortunately, the energy-resolved form of the Ehrenreich's variational result for polar optical phonon scattering is known[31] to fail for the high-temperature regime ($\sim$120 K $< T <\sim$300 K for GaAs). This would be a serious flaw since polar optical phonon scattering dominates momentum relaxation in this temperature regime except in heavily doped samples, as seen in Fig. 2. Therefore, we choose an alternative way such that we use the energy-averaged Mathiessen rule and fix the dimensionless constants to their median values, i.e., $A=4$ and $Q=1.75$. This introduces $\sim$50% uncertainty in our result for τ_s^{EY} and τ_s^{DP}. One might correct this error by directly looking into the dominant momentum relaxation process.

To calculate τ_s^{BAP}, we first need to identify the adequate regime for a given parameter set. N_c is determined by the Mott criterion[32] $N_c \approx (0.26/a_H)^3$ where $a_H = a_0\epsilon_0/(m_v/m_0)$. The thermal averaged value of $1/\tau_s^{BAP}$ is obtained as

$$\langle 1/\tau_s^{BAP}\rangle = \frac{2}{\sqrt{\pi}(k_BT)^{3/2}}\int_0^\infty \frac{1}{\tau_s^{BAP}(\epsilon)}\sqrt{\epsilon}e^{-\epsilon/k_BT}d\epsilon,$$

assuming a classical Boltzmann distribution for conduction electrons. On the other hand, the expressions for $1/\tau_s^{EY}$ and $1/\tau_s^{DP}$ in Eqs. (1) and (2) are thermally averaged with respect to ϵ. A difficulty with the calculation of τ_s^{BAP} lies in the fact that there is no reliable data for Δ_{exc}, on which τ_s^{BAP} has the dependence of $\sim 1/\Delta_{exc}^2$, for *p*-InAs and *p*-InSb. Therefore, we examine the tendency of τ_s^{BAP} as a function of Δ_{exc} as well.

IV. RESULTS AND DISCUSSION

We first compare the relative importance of each spin relaxation mechanism. Figure 3 shows the dominant spin relaxation processes for *n*-type GaAs, GaSb, InAs, and InSb. For *n*-type semiconductors, the contribution of the BAP mechanism is negligible, since the equilibrium hole concentration is extremely small. It turns out that for all materials investigated there exists a transition from the DP-dominant regime to the EY-dominant regime at $T <\sim 5$ K as the temperature is lowered. These results are consistent with the previously published results that the DP process is the relevant spin relaxation mechanism for *n*-GaAs (Refs. 19 and 22) and *n*-InAs (Ref. 21) at 300 K, and that the EY process is relevant for *n*-InSb at $T=1.3$ K.[14] When the acceptor, i.e., the minority impurity, concentration decreases, we find that the DP-dominant regime enlarges. This can be understood

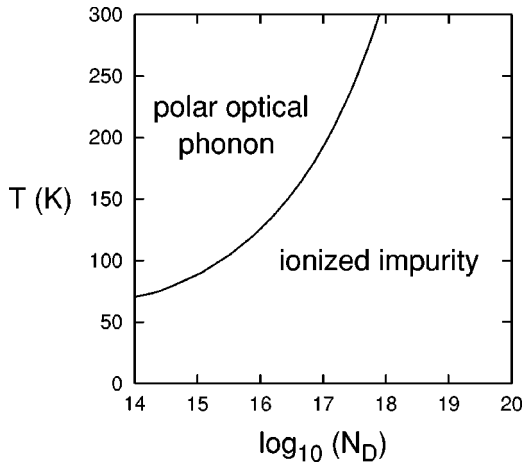

FIG. 2. Dominant momentum relaxation process for *n*-GaAs as a function of temperature and donor concentration with $N_A = 5\times10^{13}$ cm^{-3}. N_D is in cm^{-3}.

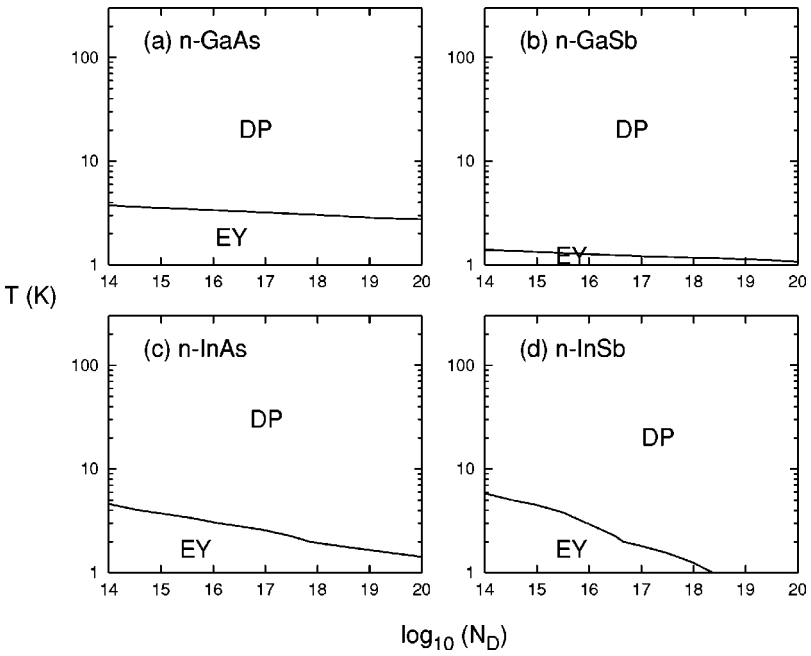

FIG. 3. Dominant spin relaxation mechanism for *n*-type materials. The higher-temperature regime is governed by the DP mechanism as shown, while the lower temperature regime is governed by the EY mechanism. N_D is in cm^{-3} and N_A is fixed to 5×10^{13} cm^{-3}. Material parameters are as specified in Table I.

from the following consideration. The acceptors in *n*-type materials are always ionized, and a decrease in the acceptor concentration corresponds to a decrease in the number of scattering centers for ionized impurity scattering, the main momentum relaxation mechanism at low temperatures. Therefore, a larger τ_p results as the acceptor concentration decreases and this induces a larger τ_s^{EY} and a smaller τ_s^{DP} since $\tau_s^{EY}\sim\tau_p$ and $\tau_s^{DP}\sim1/\tau_p$.

The diagrams for *p*-type materials are illustrated in Fig. 4 with 10^{14} $\mathrm{cm}^{-3}<N_A<10^{20}$ cm^{-3} and $N_D=5\times10^{13}$ cm^{-3}. For *p*-type materials, no systematic changes are found when the minority carrier concentration is varied. For *p*-GaAs and *p*-GaSb, we find that the BAP (DP) is dominant in the low-T (high-T) and high (low) doping regime. This is in qualitative agreement with the results of Aronov *et al.*,[12] in which similar diagrams were constructed based on experimental results. For *p*-InAs, a feature akin to those of *p*-GaAs and *p*-GaSb is found for $\Delta_{exc}=10$ μeV, and as Δ_{exc} decreases, the BAP dominant regime becomes smaller. For *p*-InSb, we obtain results similar to those for *p*-InAs as a function of Δ_{exc}. Figure 4(d) shows the case of $\Delta_{exc}=0.2$ μeV where a BAP-dominant regime exits at $T<100$ K and intermediate doping concentrations. We find abrupt discontinuities in τ_s^{BAP} at $N_A=N_c$, which results in unphysical sharp cusps at $N_A\simeq10^{18}$ cm^{-3} in Fig. 4. This is an artifact resulting from the fact that no quantitative expression for $1/\tau_s^{BAP}$ is available for the crossover between nondegenerate [Eq. (4)] and degenerate [Eq. (5)] hole regimes.

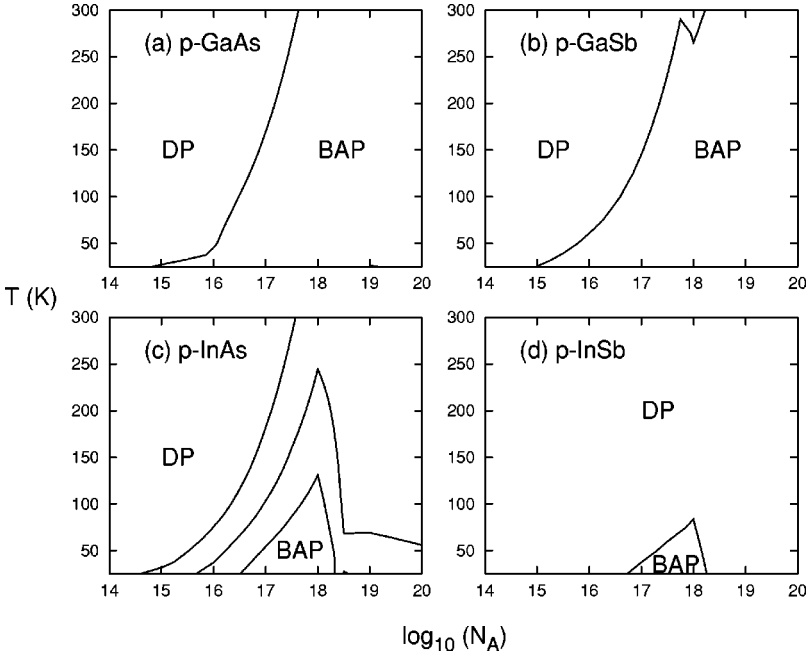

FIG. 4. Dominant spin relaxation mechanism for *p*-type materials. N_A is in cm^{-3} and N_D is fixed to 5×10^{13} cm^{-3}. The lines in (c) represent the boundaries between the DP-dominant regime and the BAP-dominant regime for $\Delta_{exc}=1$, 3 and 10 μeV from bottom to top. For *p*-InSb, Δ_{exc} is fixed at 0.2 μeV. Other material parameters including Δ_{exc} for GaAs and GaSb are as specified in Table I.

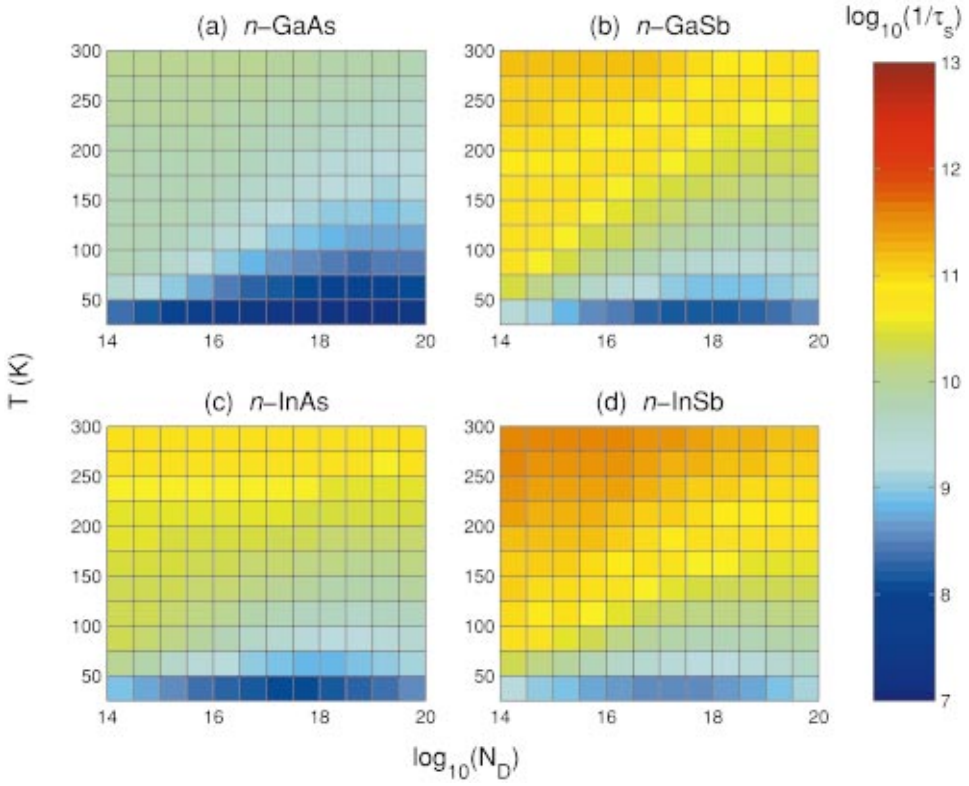

FIG. 5. (Color) Total spin relaxation time for *n*-type materials. The color of each cell represents τ_s for the point at the lower left corner of the cell according to the color map at the right-hand side. N_D is in cm^{-3} and τ_s is in second. N_A is fixed to 5×10^{13} cm^{-3}.

Experimentally, it was found that there exists an intermediate regime at $N_A \approx N_c$ where τ_s remains nearly flat with respect to the change in N_A and that the range of such an intermediate regime varies depending on the material.[12]

Figures 5 and 6 provide the total spin relaxation time $\tau_s = (1/\tau_s^{EY} + 1/\tau_s^{DP})^{-1}$ for *n*-type samples and $\tau_s = (1/\tau_s^{EY} + 1/\tau_s^{DP} + 1/\tau_s^{BAP})^{-1}$ for *p*-type samples, respectively. τ_s ranges from 1 ps to 100 ns for *n*-type materials and from 0.1

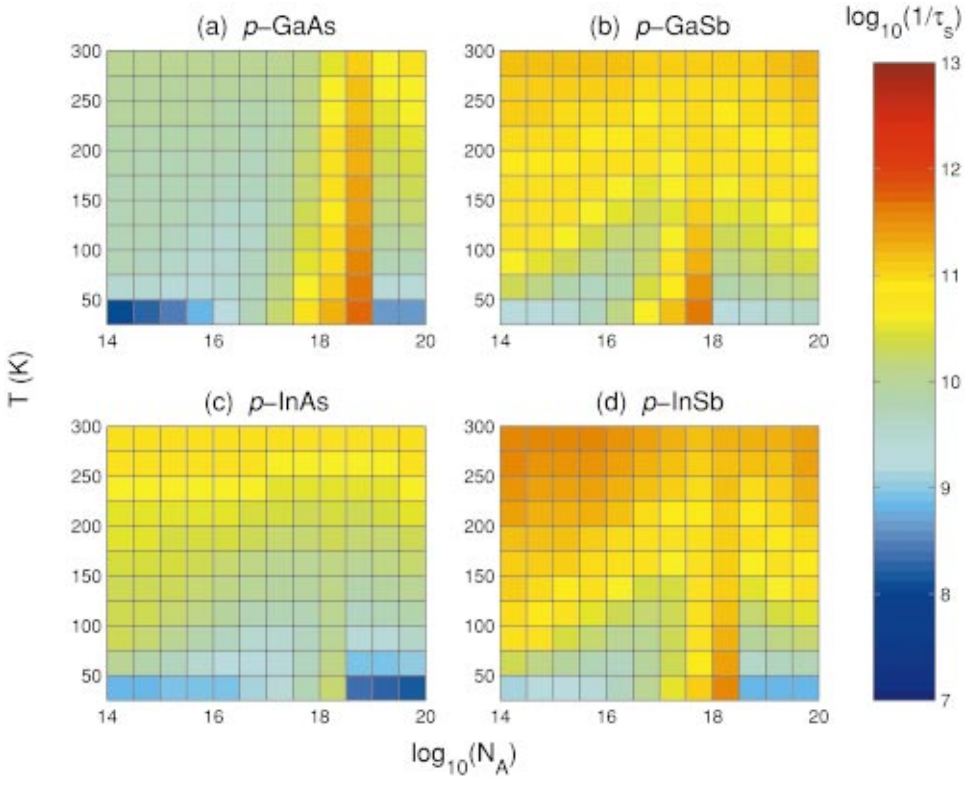

FIG. 6. (Color) Total spin relaxation time for *p*-type materials. N_A is in cm^{-3} and τ_s is in second. N_D is fixed to 5×10^{13} cm^{-3} and Δ_{exc} to 1 μeV for *p*-InAs and *p*-InSb.

ps to 10 ns for *p*-type materials, respectively, over the parameter space shown in Figs. 5 and 6. For *n*-type materials, τ_s increases as T decreases with the longest τ_s found at $N_D \sim 10^{17}-10^{18}$ cm^{-3} instead of in purer materials. This is because the regime shown in Fig. 5 is dominated solely by the DP process and $1/\tau_s^{DP}$, which is proportional to τ_p, increases as the impurity concentration decreases. The same qualitative feature has also been found in a recent experiment.[19] In our result for *n*-GaAs τ_s ranges from 5 to 60 ns for $T=25$ K, which gives a reasonable agreement with the experimental result of Ref. 19 ($\tau_s \sim 70$ ns at $T=20$ K). As for *n*-InAs with $N_D=10^{16}$ cm^{-3} and $T=300$ K, our result gives $\tau_s=12$ ps, which compares very well with a recent experimental result of $\tau_s=19\pm4$ ps.[21]

At lower temperature, we find a discrepancy with recent experimental result for *n*-GaAs. In the experiment,[19] $\tau_s \simeq 100$ ns at 5 K for $N_D=10^{16}$ cm^{-3} was reported, while our result predicts a larger value of $\tau_s \simeq 6\times10^3$ ns. Reference 19 suggested that the main spin relaxation at this low temperature regime is due to the EY mechanism. According to our result, however, since $\tau_p \sim 1$ ps and τ_s^{EY} and τ_s^{DP} are given by 7×10^4 and 6×10^3 ns, respectively, neither the EY nor DP mechanism provides a satisfactory explanation for the experimental result. Very recently,[20] a spin relaxation time of 290 ± 30 ns at 4.2 K was reported for bound electrons to donors in *n*-GaAs. The relevant spin relaxation mechanism was proposed to be the hyperfine interaction with nuclei,[38] which was not taken into account in our current work. Further research incorporating this effect is needed to resolve the discrepancy between our result and the experimental result of Ref. 19.

In *p*-type materials, a smaller τ_s, i.e., a stronger spin relaxation rate, than that in *n*-type materials is found due to the effect of the BAP process. The strong discontinuities at $N_A=N_c$ are also noticeable in Fig. 6 due to the incompleteness of the BAP expressions given by Eqs. (4) and (5), as mentioned earlier.

V. CONCLUSION

In this paper, we theoretically calculated τ_s for several bulk III-V semiconductors and compared the contributions from the three main spin relaxation mechanisms as a function of temperature and donor/acceptor concentrations. In *n*-type materials, the DP mechanism is found to be dominant down to a very low temperature, below which the EY mechanism dominates. While our calculated spin relaxation times are in reasonable agreement with the experimental results for high-temperature regime of $T>\sim20$ K, there exists a discrepancy at $T\sim5$ K for *n*-GaAs. Further theoretical efforts incorporating other spin relaxation mechanisms neglected in this paper are needed for its resolution. As for *p*-type materials, the BAP (DP) mechanism is dominant at low (high) temperature and high (low) acceptor concentrations. We find that the crossover between various regimes for spin relaxation requires further theoretical investigation for a more thorough understanding and realistic comparison with experimental data. This is especially the case for the crossover between nondegenerate and degenerate hole regimes for the BAP process.

ACKNOWLEDGMENTS

We are thankful to M. I. D'yakonov for critical comments and to J. M. Kikkawa for useful discussion. This work was supported by the Office of Naval Research and the Defense Advanced Research Projects Agency.

*Electronic address: kwk@eos.ncsu.edu

[1] D. DiVincenzo, Science **270**, 255 (1995).
[2] G. Prinz, Science **282**, 1660 (1998).
[3] L. Sham, Science **277**, 1258 (1997).
[4] R. J. Elliot, Phys. Rev. **96**, 266 (1954).
[5] Y. Yafet, in *Solid State Physics*, edited by F. Seitz and D. Turnbull (Academic, New York, 1963), Vol. 14.
[6] M. I. D'yakonov and V. I. Perel, Zh. Éksp. Teor. Fiz. **60**, 1954 (1971) [Sov. Phys. JETP **33**, 1053 (1971)]; Fiz. Tverd. Tela (Leningrad) **13**, 3581 (1971) [Sov. Phys. Solid State **13**, 3023 (1972)].
[7] G. L. Bir, A. G. Aronov, and G. E. Pikus, Zh. Éksp. Teor. Fiz. **69**, 1382 (1975) [Sov. Phys. JETP **42**, 705 (1976)].
[8] A. H. Clark, R. D. Burnham, D. J. Chadi, and R. M. White, Solid State Commun. **20**, 385 (1976).
[9] G. Fishman and G. Lampel, Phys. Rev. B **16**, 820 (1977).
[10] V. I. Maruschak, M. N. Stepanova, and A. N. Titkov, Fiz. Tverd. Tela (Lenningrad) **25**, 3537 (1983) [Sov. Phys. Solid State **25**, 2035 (1983)].
[11] K. Zerrouati, F. Fabre, G. Bacquet, J. Bandet, J. Frandon, G. Lampel, and D. Paget, Phys. Rev. B **37**, 1334 (1988).
[12] A. G. Aronov, G. E. Pikus, and A. N. Titkov, Zh. Éksp. Teor. Fiz. **84**, 1170 (1983) [Sov. Phys. JETP **57**, 680 (1983)].
[13] A. H. Clark, R. D. Burnham, D. J. Chadi, and R. M. White, Phys. Rev. B **12**, 5758 (1975).
[14] J. N. Chazalviel, Phys. Rev. B **11**, 1555 (1975).
[15] Y. Ohno, R. Terauchi, T. Adachi, F. Matsukura, and H. Ohno, Phys. Rev. Lett. **83**, 4196 (1999).
[16] K. C. Hall, S. W. Leonard, H. M. van Driel, A. R. Kost, E. Selvig, and D. H. Chow, Appl. Phys. Lett. **75**, 4156 (1999).
[17] J. T. Hyland, G. T. Kennedy, A. Miller, and C. C. Button, Semicond. Sci. Technol. **14**, 215 (1999).
[18] A. Malinowski, R. S. Britton, T. Grevatt, R. T. Harley, D. A. Ritchie, and M. Y. Simmons, Phys. Rev. B **62**, 13 034 (2000).
[19] J. M. Kikkawa and D. D. Awschalom, Phys. Rev. Lett. **80**, 4313 (1998).
[20] R. I. Dzhioev, B. P. Zakharchenya, V. L. Korenev, D. Gammon, and D. S. Katzer, Pis'ma Zh. Éksp. Teor. Fiz. **74**, 200 (2001) [JETP Lett. **74**, 182 (2001).
[21] T. F. Boggess, J. T. Olesberg, C. Yu, M. E. Flatté, and W. H. Lau, Appl. Phys. Lett. **77**, 1333 (2000).
[22] W. H. Lau, J. T. Olesberg, and M. E. Flatté, Phys. Rev. B **64**, 161 301 (2001).
[23] M. Z. Maialle, Phys. Rev. B **54**, 1967 (1996); M. Z. Maialle and M. H. Degani, Appl. Phys. Lett. **70**, 1864 (1997); Phys. Rev. B **55**, 13 771 (1997).

[24] G. E. Pikus and A. N. Titkov, in *Optical Orientation*, edited by F. Meier and B. P. Zakharchenya (North-Holland, Amsterdam, 1984).
[25] H. Ehrenreich, Phys. Rev. B **120**, 1951 (1960).
[26] H. Ehrenreich, J. Phys. Chem. Solids **8**, 130 (1959).
[27] H. Brooks, Adv. Electron. Electron Phys. **7**, 158 (1955).
[28] H. J. G. Meijer and D. Polder, Physica (Amsterdam) **19**, 255 (1953).
[29] J. D. Zook, Phys. Rev. **136**, A869 (1964).
[30] J. Bardeen and W. Shockley, Phys. Rev. **80**, 72 (1950).
[31] H. Ehrenreich, J. Appl. Phys. **32**, 2155 (1961).
[32] P. P. Edwards and M. J. Sienko, Phys. Rev. B **17**, 2575 (1978).
[33] D. L. Rode and S. Knight, Phys. Rev. B **3**, 2534 (1971).
[34] D. L. Rode, Phys. Rev. B **3**, 3287 (1971).
[35] *Numerical Data and Functional Relationships in Science and Technology*, edited by O. Madelung, M. Schultz, and H. Weiss, Landolt-Bornstein, New Series, Group III, Vol. 17, Pt. a (Springer-Berlin,1982); *Semiconductors—Basic Data*, 2nd ed., edited by O. Madelung (Springer, New York, 1996).
[36] E. Haga and H. Kimura, J. Phys. Soc. Jpn. **19**, 658 (1964).
[37] D. D. Sell, Surf. Sci. **35**, 863 (1973).
[38] A. Abragam, *The Principles of Nuclear Magnetism* (Clarendon, Oxford, 1961).